Struct Multidisc Optim (2010) 42:869–877
DOI 10.1007/s00158-010-0525-7

RESEARCH PAPER

Michell cantilevers constructed within a half strip. Tabulation of selected benchmark results

Cezary Graczykowski · Tomasz Lewiński

Received: 8 April 2010 / Revised: 18 May 2010 / Accepted: 24 May 2010 / Published online: 3 July 2010

Abstract The paper delivers the benchmark results for the Michell cantilevers constructed within a half strip, for selected values of the σ_T/σ_C ratio, σ_T, σ_C being the admissible stresses in tension and compression, respectively.

Keywords Michell structures · Minimum weight design · Topology optimization · Trusses

1 Introduction

The aim of the present paper is to deliver a family of analytical solutions to Michell's problem: find the lightest framework lying within the half strip: $x'' > 0$, $-\frac{a}{2} \leqslant y'' \leqslant \frac{a}{2}$, transmitting a given vertical force of magnitude P applied at point P of coordinates $(x'_p,\ y''_p)$—to the support RN, see Fig. 1. The axial stress σ must satisfy the bounding conditions:

$$-\sigma_C \leqslant \sigma \leqslant \sigma_T$$

C. Graczykowski (✉)
Institute of Fundamental Technological Research,
Polish Academy of Sciences, Ul. Pawińskiego 5b,
02-106 Warsaw, Poland
e-mail: Cezary.Graczykowski@ippt.gov.pl

T. Lewiński
Department of Structural Mechanics and Computer Aided Engineering, Faculty of Civil Engineering,
Warsaw University of Technology, Al.Armii Ludowej 16,
00-637 Warsaw, Poland
e-mail: T.Lewinski@il.pw.edu.pl

The problem above has been set by Prager (1959). The analytical study of this problem can be found in Rozvany (1997) and in Graczykowski and Lewiński (2006a, b, c, 2007a, b). Unfortunately, the latter study omitted the paper by Srithongchai and Dewhurst (2003), including some analytical results concerning the case of point P lying close to RN with the conditions: $-\frac{a}{2} \leqslant y''_p \leqslant \frac{a}{2}$ being nonactive.

The topology optimization programs developed in recent years need to be verified by Michell- like benchmarks. That is why it is thought appropriate to set up and tabulate the optimal layouts of the problem discussed here for many selected positions of point P and for many values of the $\frac{\sigma_C}{\sigma_T}$ ratio. Such tabulation requires an additional program. Its algorithm will be explained in the sequel.

Michell's structures are determined by Hencky's nets $(\alpha,\ \beta)$ introduced in Carathéodory and Schmidt (1923). In the present paper the point P of application of the force $\boldsymbol{P}$ is given by its Cartesian coordinates $(x''_p,\ y''_p)$. Thus our aim is to find an algorithm which determines the curvilinear coordinates $(\alpha_p,\ \beta_p)$ of point P by means of the Cartesian coordinates $(x''_p,\ y''_p)$. Such an algorithm is fairly complex, since the feasible domain—here the half strip—is composed of many subdomains referring to specific forms of the analytical solution, see Fig. 19 in Graczykowski and Lewiński (2006a). The division of the half strip into subdomains is a consequence of the governing equations of the Hencky nets being hyperbolic.

The present paper extends the results of Section 4 of Graczykowski and Lewiński (2006c), where some selected values of volumes of the optimal cantilevers corresponding to $\frac{\sigma_T}{\sigma_C} = 3$ and to $y''_p = 0$, $0 \leqslant x''_p \leqslant 3a$ have been tabulated.

The plan of the paper is the following. First, we develop a method of finding $(\alpha_p,\ \beta_p)$ for arbitrary position of point P in the half strip considered. We show details of the subdivision of this domain for selected values of $\kappa = \frac{\sigma_T}{\sigma_C}$. In the

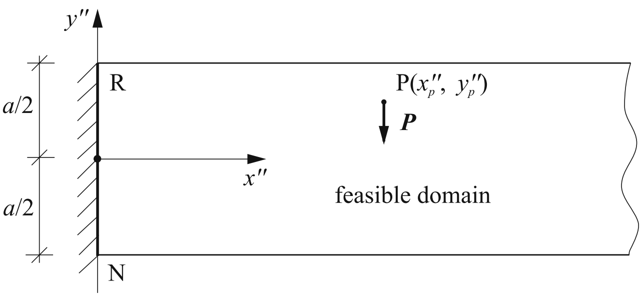

Fig. 1 Formulation of the problem

second step we deliver the analytical formulae expressing the virtual displacements and, consequently, the formulae for the volumes of the optimal cantilevers. These volumes are normalized with respect to $V_0 = \frac{Pa}{\sigma_T}$.

We use the notation of the papers: Graczykowski and Lewiński (2006a, b, c, 2007a, b), used also in Lewiński et al. (1994a, b) and Hemp (1973). The following convention is adopted: notation (a.4.5), Section a.4 means (4.5), Section 4 of Graczykowski and Lewiński (2006a). Similarly, (b.2.3), Section b.2 means (2.3), Section 2 of Graczykowski and Lewiński (2006b).

2 Determination of the curvilinear coordinates (α, β) of a point (x'', y'')

The half strip of Fig. 1 is parameterized by the Cartesian systems (x'', y''), (x', y'), (x, y) as explained in Fig. 2. Given are: $|\mathrm{RN}| = a$, $\kappa = \frac{\sigma_T}{\sigma_C}$. Position of point P of application of the vertical (or parallel to y'') force of magnitude P is given by (x''_p, y''_p). The domain $x'' \geqslant 0$, $-\frac{a}{2} \leqslant y'' \leqslant \frac{a}{2}$ is divided into the following subdomains, see Graczykowski and Lewiński (2006a).

a) domain I or RAN

This is the right angled triangle RAN of angles γ_1, γ_2 given by $\gamma_1 = \arctan(\kappa^{\frac{1}{2}})$, $\gamma_2 = \frac{\pi}{2} - \gamma_1$ and of sides: $r_1 = a\cos\gamma_1$,

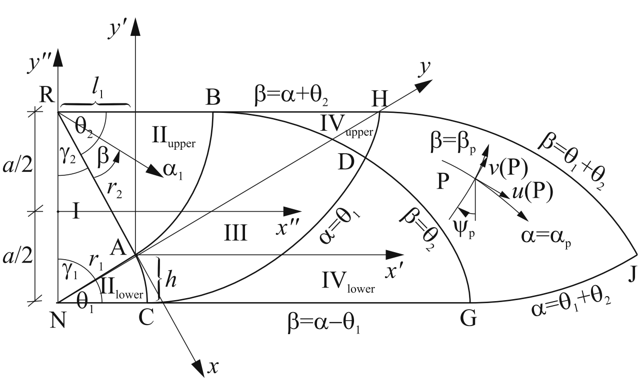

Fig. 2 Geometry of the Michell cantilever

$r_2 = a\sin\gamma_1$. Note that $\frac{r_2}{r_1} = \kappa^{\frac{1}{2}}$, $\theta_2 = \frac{\pi}{2} - \gamma_2$, $\theta_1 = \frac{\pi}{2} - \gamma_1$. Point A has the Cartesian coordinates: $x'' = l_1$, $y'' = -\left(\frac{a}{2} - h\right)$, where $l_1 = r_2\cos\gamma_1$ and $h = r_1\cos\gamma_1$. Point A is the origin of two new Cartesian frames: (x', y') parallel to (x'', y'') and of the rotated frame (x, y) determined by RA and NA. These coordinates are interrelated by $x'' = x' + l_1$, $y'' = y' - \left(\frac{a}{2} - h\right)$ or

$$x'' = x'a\sin\gamma_1\cos\gamma_1, \qquad y'' = y' - \frac{a}{2} + a\cos^2\gamma_1 \tag{1}$$

and

$$x = x'\cos\gamma_1 - y'\sin\gamma_1, \qquad y = x'\sin\gamma_1 + y'\cos\gamma_1 \tag{2}$$

By (1), (2) one finds

$$\begin{aligned} x &= (x'' - a\sin\gamma_1\cos\gamma_1)\cos\gamma_1 + \\ &\quad - \left(y'' + \frac{a}{2} - a\cos^2\gamma_1\right)\sin\gamma_1 \\ y &= (x'' - a\sin\gamma_1\cos\gamma_1)\sin\gamma_1 + \\ &\quad + \left(y'' + \frac{a}{2} - a\cos^2\gamma_1\right)\cos\gamma_1 \end{aligned} \tag{3}$$

If P lies within domain I the solution is a two bar truss of bars parallel RA and NA, see Section a.4. This case will not be discussed in the present paper.

b) domain II_{upper} or RAB

We introduce the polar coordinates (α_1, β) such that $\alpha_1 r_2$ represents the distance to R and β is an angle measured from RA, see Fig. a.7. Having (x''_p, y''_p) of an arbitrary point P within RAB we compute

$$\beta_p = \arctan\left(\frac{x''_p}{\frac{a}{2} - y''_p}\right) - \gamma_2,$$

$$(\alpha_1)_p = \frac{x''_p}{r_2\sin(\beta_p + \gamma_2)} \tag{4}$$

c) domain II_{lower} or NAC

We introduce the polar coordinates (α, β_1) such that $\beta_1 r_1$ is the distance to N and angle α is measured from the line NA, see Fig. a.8. The polar coordinates of point (x''_p, y''_p) can be found by

$$\alpha_p = \arctan\left(\frac{x''_p}{\frac{a}{2} + y''_p}\right) - \gamma_1,$$

$$(\beta_1)_p = \frac{x''_p}{r_1\sin(\alpha_p + \gamma_1)} \tag{5}$$

d) domain III or ABDC

This domain will be called Prager-Hill domain. Its parameterization $(\alpha,\ \beta)$ is explained in Section a.6. The equations $x = x(\alpha,\ \beta)$, $y = y(\alpha,\ \beta)$ are given by (a.6.15, a.6.16). These equations along with (3) interrelate $(x'',\ y'')$ with $(\alpha,\ \beta)$. Having $(x''_p,\ y''_p)$ of point P lying within this domain one can recover its curvilinear coordinates $(\alpha_p,\ \beta_p)$ by solving this nonlinear algebraic system. The $(\alpha,\ \beta)$ coordinates of point D are $(\theta_1,\ \theta_2)$.

e) domain IV_{upper} or BDH

This domain, called Chan-like domain in Section a.7, is parameterized by $(\alpha,\ \beta)$ This parameterization becomes singular along BH where $\beta - \alpha = \theta_2$, where the Lamé coefficient B vanishes. The equations (a.7.30) and (a.6.16) determine the shapes of the parametric lines α and β. By using (3) and these equations one can recover the $(\alpha_p,\ \beta_p)$. coordinates of an arbitrary point $(x''_p,\ y''_p)$ lying within this domain. The $(\alpha,\ \beta)$ coordinates of point H are $(\theta_1,\ \theta_1 + \theta_2)$.

f) domain IV_{lower} or CDG

The procedure is based on (a.7.18, a.7.19) and (3). The $(\alpha,\ \beta)$ coordinates of point G are $(\theta_1 + \theta_2,\ \theta_2)$.

g) domain V or DHJG

The parametric lines $x(\alpha,\ \beta)$, $y(\alpha,\ \beta)$ are given by (a.8.5), (a.6.16). To recover $(\alpha_p,\ \beta_p)$ having $(x''_p,\ y''_p)$ one should use (3). The $(\alpha,\ \beta)$ coordinates of point J are $(\theta_1 + \theta_2,\ \theta_1 + \theta_2)$.

We shall not consider the cases of points P lying in domains VI_{upper}, VI_{lower} and further, see Fig. a.19.

The procedure of determination of $(\alpha,\ \beta)$ coordinates of points of Cartesian coordinates $(x'',\ y'')$ within the domain RBHJGCNR of Fig. 2 has been written in Maple using the formulae above. The program is executed for a fixed grid of points $(x''_p,\ y''_p)$ for fixed $\kappa > 0$. Computation of $(\alpha_p,\ \beta_p)$ is preceded by detection to which domain the point $(x''_p,\ y''_p)$ belongs, which determines further computation.

The value of κ determines the net of lines $(\alpha,\ \beta)$ and position of nodes A, B, C, D, H, G, J. Given $(x''_p,\ y''_p)$ we cut out the optimal cantilever following the lines $\alpha_p = \text{const}$ and $\beta_p = \text{const}$.

The solution is characterized not only by the parametric lines $(\alpha,\ \beta)$ but also by the Lamé coefficients $A(\alpha,\ \beta)$, $B(\alpha,\ \beta)$, the force fields $T_1(\alpha,\ \beta)$, $T_2(\alpha,\ \beta)$ and the density of the fibres $h(\alpha,\ \beta)$, see Graczykowski and Lewiński (2006b, 2007a, b). It is impossible to give here all these

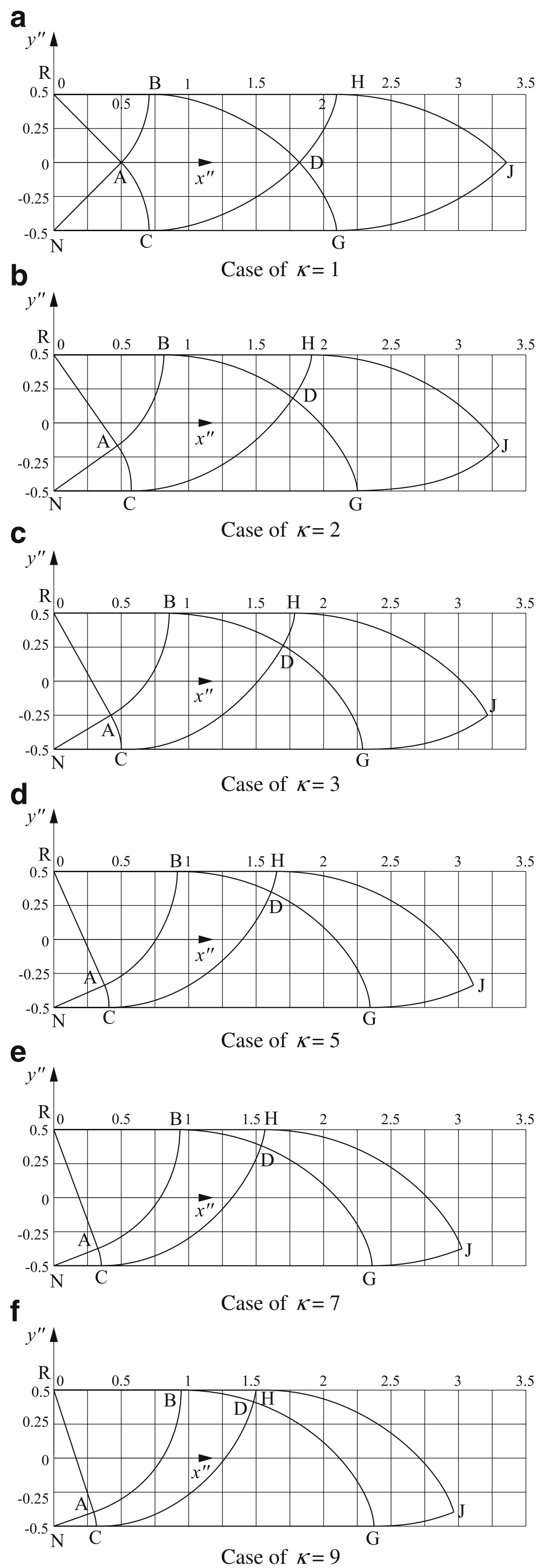

Fig. 3 **a** Case of $\kappa = 1$, **b** Case of $\kappa = 2$, **c** Case of $\kappa = 3$, **d** Case of $\kappa = 5$, **e** Case of $\kappa = 7$, **f** Case of $\kappa = 9$

Table 1 Coordinates of points A, B, C, D, H, G, J

κ	$x''(A)$	$y''(A)$	$x''(B)$	$x''(C)$	$x''(D)$	$y''(D)$	$x''(H)$	$x''(G)$	$x''(J)$	$y''(J)$
1	0.5000	0.0000	0.7071	0.7071	1.8220	0.0000	2.0971	2.0971	3.3589	0.0000
2	0.4714	−0.1667	0.8165	0.5774	1.7728	0.1749	1.9096	2.2395	3.3025	−0.1704
3	0.4330	−0.2500	0.8660	0.5000	1.7072	0.2608	1.7920	2.2966	3.2272	−0.2548
5	0.3727	−0.3333	0.9129	0.4082	1.6051	0.3448	1.6489	2.3442	3.1096	−0.3383
7	0.3307	−0.3750	0.9354	0.3536	1.5348	0.3857	1.5624	2.3641	3.0283	−0.3795
9	0.3000	−0.4000	0.9487	0.3162	1.4837	0.4097	1.5031	2.3747	2.9691	−0.4040

details. Integration of $h(\alpha, \ \beta)$ over a cantilever area gives the volume V. The same value of V can be obtained by the kinematic method, see (a.2.12). This method is outlined in the next section.

Table 2 The coordinates of point P and the volumes of the optimal cantilevers. Case of $\kappa = 1$

x''_p/a	y''_p/a	Subdomain	V/V_0
0.25	0.5	RBA	0.642699081
0.5	0.5	RBA	1.285398163
0.75	0.5	BDH	1.930991655
1	0.5	BDH	2.70027166
1.25	0.5	BDH	3.640051786
1.5	0.5	BDH	4.729085649
1.75	0.5	BDH	5.949111345
2	0.5	BDH	7.284800436
0.5	0.25	RBA	1.071750554
0.75	0.25	ABDC	1.7079837
1	0.25	ABDC	2.503274786
1.25	0.25	ABDC	3.460899678
1.5	0.25	ABDC	4.551598331
1.75	0.25	BDH	5.76349763
2	0.25	BDH	7.092246275
2.25	0.25	DHJG	8.540766317
2.5	0.25	DHJG	10.1205242
2.75	0.25	DHJG	11.82731937
3	0.25	DHJG	13.65864691
0.75	0	ABDC	1.615270799
1	0	ABDC	2.427657745
1.25	0	ABDC	3.397942742
1.5	0	ABDC	4.498115388
1.75	0	ABDC	5.707748253
2	0	DHJG	7.024707829
2.25	0	DHJG	8.475913799
2.5	0	DHJG	10.05771892
2.75	0	DHJG	11.76573462
3	0	DHJG	13.59718555
3.25	0	DHJG	15.55137495

3 Computation of the volumes of the optimal cantilevers

The volume of the optimal cantilever is computed by

$$V = \frac{w_p}{a} V_0, \qquad V_0 = \frac{Pa}{\sigma_T} \tag{6}$$

Here w_p is the vertical virtual displacement of point P; $w_p > 0$ if directed along the vertical force $\boldsymbol{P}$. Since $u(\mathrm{P})$, $v(\mathrm{P})$ are virtual displacements of point P, measured along the lines α and β, the displacement w_p equals

$$w_p = u(\mathrm{P}) \sin \psi_p - v(\mathrm{P}) \cos \psi_p, \tag{7}$$

see (2.11) in Graczykowski and Lewiński (2007b). Here ψ_p represents an angle between tangent to the β-line and y'' axis, see Fig. 2.

Domain RAB Assume that point P of given coordinates $(x''_p, \ y''_p)$ lies within RAB. The optimal structure is composed of a circular fan reinforced by a circular bar which becomes straight within the RAN domain. The volume of this optimal structure is given by (6), (7) with

$$\begin{aligned} u(\mathrm{P}) &= r_2(\alpha_1)_p, \\ v(\mathrm{P}) &= -(\kappa+1) r_2(\alpha_1)_p \beta_p - \kappa r_1(\alpha_1)_p, \\ \psi_p &= \frac{\pi}{2} - \gamma_2 - \beta_p \end{aligned} \tag{8}$$

see (b.4.5). The coordinates $(\alpha_1)_p$ are determined by (4).

Domain NAC The optimal structure is similar to the previous one. The volume is given by (6) and (7), where

$$\begin{aligned} u(\mathrm{P}) &= (\kappa+1)\alpha_p r_1(\beta_1)_p + r_2(\beta_1)_p, \\ v(\mathrm{P}) &= -\kappa r_1(\beta_1)_p, \\ \psi_p &= \gamma_1 + \alpha_p \end{aligned} \tag{9}$$

and α_p, $(\beta_1)_p$ are computed by (5).

Domain ABDC The optimal structure is composed of two circular fans and the net in ABDC. The structure is

Table 3 The coordinates of point P and the volumes of the optimal cantilevers. Case of $\kappa = 2$

x''_p/a	y''_p/a	Subdomain	V/V_0
0.25	0.5	RBA	1.070040854
0.5	0.5	RBA	2.140081709
0.75	0.5	RBA	3.210122564
1	0.5	BDH	4.352323536
1.25	0.5	BDH	5.736280925
1.5	0.5	BDH	7.340969479
1.75	0.5	BDH	9.139706374
0.25	0.25	RBA	0.7309922318
0.5	0.25	RBA	1.694610296
0.75	0.25	RBA	2.736183815
1	0.25	ABDC	3.904765147
1.25	0.25	ABDC	5.322079688
1.5	0.25	ABDC	6.942821578
1.75	0.25	BDH	8.735189594
2	0.25	DHJG	10.7072414
2.25	0.25	DHJG	12.88253804
2.5	0.25	DHJG	15.25484812
2.75	0.25	DHJG	17.81832457
0.5	0	RBA	1.461984463
0.75	0	ABDC	2.406968418
1	0	ABDC	3.614969202
1.25	0	ABDC	5.061295781
1.5	0	ABDC	6.70293968
1.75	0	CDG	8.513436936
2	0	DHJG	10.49966444
2.25	0	DHJG	12.67443499
2.5	0	DHJG	15.04550743
2.75	0	DHJG	17.60644946
3	0	DHJG	20.3533315
0.5	−0.25	NAC	1.43485493
0.75	−0.25	ABDC	2.346467223
1	−0.25	ABDC	3.548592388
1.25	−0.25	ABDC	4.987575453
1.5	−0.25	CDG	6.62904138
1.75	−0.25	CDG	8.468258943
2	−0.25	CDG	10.48419477
2.25	−0.25	DHJG	12.66096962
2.5	−0.25	DHJG	15.02493855
2.75	−0.25	DHJG	17.58003486
3	−0.25	DHJG	20.32236606
0.25	−0.5	NAC	0.815163172
0.5	−0.5	NAC	1.630326344
0.75	−0.5	CDG	2.519807744
1	−0.5	CDG	3.688468456
1.25	−0.5	CDG	5.115806891
1.5	−0.5	CDG	6.769254805
1.75	−0.5	CDG	8.620909074
2	−0.5	CDG	10.64740795

Table 4 The coordinates of point P and the volumes of the optimal cantilevers. Case of $\kappa = 3$

x''_p/a	y''_p/a	Subdomain	V/V_0
0.25	0.5	RBA	1.480210253
0.5	0.5	RBA	2.960420506
0.75	0.5	RBA	4.440630759
1	0.5	BDH	5.970732623
1.25	0.5	BDH	7.793958822
1.5	0.5	BDH	9.908893565
1.75	0.5	BDH	12.28053401
0.25	0.25	RBA	0.9448120897
0.5	0.25	RBA	2.283125287
0.75	0.25	RBA	3.725379095
1	0.25	ABDC	5.27560944
1.25	0.25	ABDC	7.144439672
1.5	0.25	ABDC	9.286811415
1.75	0.25	DHJG	11.65799565
2	0.25	DHJG	14.28482994
2.25	0.25	DHJG	17.18514923
2.5	0.25	DHJG	20.34875837
0.5	0	RBA	1.889624179
0.75	0	ABDC	3.181196473
1	0	ABDC	4.774132805
1.25	0	ABDC	6.687102239
1.5	0	ABDC	8.861233022
1.75	0	CDG	11.27758404
2	0	CDG	13.93605154
2.25	0	DHJG	16.83306687
2.5	0	DHJG	19.99191059
2.75	0	DHJG	23.4049224
3	0	DHJG	27.06729759
0.5	−0.25	ABDC	1.749659095
0.75	−0.25	ABDC	2.965862342
1	−0.25	ABDC	4.564952533
1.25	−0.25	CDG	6.445490122
1.5	−0.25	CDG	8.670713056
1.75	−0.25	CDG	11.13298039
2	−0.25	CDG	13.83152805
2.25	−0.25	DHJG	16.74071406
2.5	−0.25	DHJG	19.88746058
2.75	−0.25	DHJG	23.29002352
3	−0.25	DHJG	26.94341138
0.25	−0.5	NAC	0.9566114773
0.5	−0.5	NAC	1.913222955
0.75	−0.5	CDG	3.083593618
1	−0.5	CDG	4.648662656
1.25	−0.5	CDG	6.560007435
1.5	−0.5	CDG	8.773874677
1.75	−0.5	CDG	11.25282072
2	−0.5	CDG	13.96552371
2.25	−0.5	CDG	16.8859507

Table 5 The coordinates of point P and the volumes of the optimal cantilevers. Case of $\kappa = 5$

x''_p/a	y''_p/a	Subdomain	V/V_0
0.25	0.5	RBA	2.284409983
0.5	0.5	RBA	4.568819966
0.75	0.5	RBA	6.853229949
1	0.5	BDH	9.168419313
1.25	0.5	BDH	11.86391644
1.5	0.5	BDH	14.99250407
0.25	0.25	RBA	1.356312737
0.5	0.25	RBA	3.427877137
0.75	0.25	RBA	5.655352453
1	0.25	ABDC	7.98146982
1.25	0.25	ABDC	10.74448251
1.5	0.25	ABDC	13.92074013
1.75	0.25	CDG	17.46356037
2	0.25	DHJG	21.40196207
2.25	0.25	DHJG	25.75088019
2.5	0.25	DHJG	30.49646567
0.25	0	RBA	1.123686906
0.5	0	RBA	2.712625475
0.75	0	RBA	4.707218232
1	0	ABDC	7.059621036
1.25	0	ABDC	9.895552532
1.5	0	CDG	13.13188174
1.75	0	CDG	16.76665737
2	0	CDG	20.76569836
2.25	0	DHJG	25.10927853
2.5	0	DHJG	29.8426122
2.75	0	DHJG	34.95961695
0.5	−0.25	RBA	2.370438795
0.75	−0.25	ABDC	4.183325622
1	−0.25	ABDC	6.564796573
1.25	−0.25	CDG	9.371501384
1.5	−0.25	CDG	12.7194026
1.75	−0.25	CDG	16.42363692
2	−0.25	CDG	20.4830012
2.25	−0.25	CDG	24.85780627
2.5	−0.25	DHJG	29.56920948
2.75	−0.25	DHJG	34.66641774
3	−0.25	DHJG	40.14280544
0.25	−0.5	NAC	1.189818497
0.5	−0.5	CDG	2.425684518
0.75	−0.5	CDG	4.186758048
1	−0.5	CDG	6.541823935
1.25	−0.5	CDG	9.417783331
1.5	−0.5	CDG	12.74865265
1.75	−0.5	CDG	16.47800871
2	−0.5	CDG	20.55868265
2.25	−0.5	CDG	24.95148939

Table 6 The coordinates of point P and the volumes of the optimal cantilevers. Case of $\kappa = 7$

x''_p/a	y''_p/a	Subdomain	V/V_0
0.25	0.5	RBA	3.080296234
0.5	0.5	RBA	6.160592468
0.75	0.5	RBA	9.240888702
1	0.5	BDH	12.34341583
1.25	0.5	BDH	15.90727283
1.5	0.5	BDH	20.04526852
0.25	0.25	RBA	1.759499907
0.5	0.25	RBA	4.556002031
0.75	0.25	RBA	7.560385369
1	0.25	ABDC	10.66629332
1.25	0.25	ABDC	14.31847766
1.5	0.25	CDG	18.52370494
1.75	0.25	CDG	23.24946117
2	0.25	DHJG	28.49964853
2.25	0.25	DHJG	34.29670701
0.25	0	RBA	1.365998797
0.5	0	RBA	3.518999813
0.75	0	RBA	6.212873078
1	0	ABDC	9.325684314
1.25	0	ABDC	13.07876552
1.5	0	CDG	17.38479457
1.75	0	CDG	22.23619405
2	0	CDG	27.5736446
2.25	0	DHJG	33.36436052
2.5	0	DHJG	39.67198242
2.75	0	DHJG	46.49342052
0.5	−0.25	RBA	2.979417573
0.75	−0.25	ABDC	5.388180925
1	−0.25	ABDC	8.545432199
1.25	−0.25	CDG	12.28217819
1.5	−0.25	CDG	16.75083932
1.75	−0.25	CDG	21.69497402
2	−0.25	CDG	27.11295079
2.25	−0.25	CDG	32.95178334
2.5	−0.25	DHJG	39.22869403
2.75	−0.25	DHJG	46.02082353
0.25	−0.5	NAC	1.384172076
0.5	−0.5	CDG	2.927039232
0.75	−0.5	CDG	5.277790785
1	−0.5	CDG	8.421445305
1.25	−0.5	CDG	12.26032085
1.5	−0.5	CDG	16.70627391
1.75	−0.5	CDG	21.68395282
2	−0.5	CDG	27.13037838
2.25	−0.5	CDG	32.99324017

reinforced by bars along RBD and NCD. The volume is given by (6) and (7), where

$$u(\mathrm{P}) = u^*(\alpha_p,\ \beta_p), \qquad v(\mathrm{P}) = v^*(\alpha_p,\ \beta_p),$$
$$\psi_p = \gamma_1 + \alpha_p - \beta_p \tag{10}$$

where $(\alpha_p,\ \beta_p)$ are recovered from $(x''_p,\ y''_p)$ as explained in Section 2; the functions u^*, v^* were defined in Section b.5 by (b.5.11b), (b.5.6b).

Domain BDH Now point P lies within BDH. The upper reinforcing bar will be partly straight along BH and there its area is not constant. The lower reinforcing bar is prismatic. Examples of such structures can be found in Graczykowski and Lewiński (2007b). The volume is given by (6), (7), where ψ_p is given by (10) and

$$u(\mathrm{P}) = u^*(\alpha_p,\ \beta_p) + u^\bullet(\alpha_p + \theta_2,\ \beta_p - \theta_2),$$

$$v(\mathrm{P}) = v^*(\alpha_p,\ \beta_p) + v^\bullet(\alpha_p + \theta_2,\ \beta_p - \theta_2). \tag{11}$$

Here u^*, v^* are defined as above, while

$$\frac{u^\bullet(\xi,\ \eta)}{r_1} = -(\kappa+2)F_3(\eta,\xi) - \kappa F_1(\eta,\xi) - 2\kappa^{\frac{1}{2}}F_2(\eta,\xi)$$
$$-(\kappa+1)\xi\left[G_2(\eta,\xi) + \kappa^{\frac{1}{2}}G_1(\eta,\xi)\right] \tag{12}$$

and $v^\bullet(\xi,\ \eta)$ has been defined by (b.6.31).

Domain CDG The optimal structure will be similar to the previous one. The volume is given by (6), (7) with ψ_p given by (10) and

$$u(\mathrm{P}) = u^*(\alpha_p,\ \beta_p) + u_\bullet(\alpha_p - \theta_1,\ \beta_p + \theta_1)$$

$$v(\mathrm{P}) = v^*(\alpha_p,\ \beta_p) + v_\bullet(\alpha_p - \theta_1,\ \beta_p + \theta_1) \tag{13}$$

Where u^*, v^* were given by (b.5.11b), (b.5.6b) and

$$\frac{u_\bullet(\xi,\eta)}{r_1} = \kappa F_1(\xi,\eta) + 2\kappa^{\frac{3}{2}}F_2(\xi,\eta) - \kappa F_3(\xi,\eta)$$
$$-(\kappa+1)\xi\left[G_o(\xi,\eta) + \kappa^{\frac{1}{2}}G_1(\xi,\eta)\right] \tag{14}$$

and $v_\bullet(\xi,\ \eta)$ has been given by (b.6.15).

Domain DHJG Point P of coordinates $(x''_p,\ y''_p)$ lies within DHJG. The coordinates $(\alpha_p,\ \beta_p)$ can be computed as explained in Section 2. Exemplary optimal cantilevers belonging to this class are discussed in Graczykowski and Lewiński (2007b). Their volume is given by (6), (7) with ψ_p given by (10); the virtual displacements of point P are expressed by

$$u(\mathrm{P}) = u^*(\alpha_p,\ \beta_p) + u_\bullet(\alpha_p - \theta_1,\ \beta_p + \theta_1)$$
$$+ u^\bullet(\alpha_p + \theta_2,\ \beta_p - \theta_2) \tag{15}$$

Table 7 The coordinates of point P and the volumes of the optimal cantilevers. Case of $\kappa = 9$

x''_p/a	y''_p/a	Subdomain	V/V_0
0.25	0.5	RBA	3.872614432
0.5	0.5	RBA	7.745228864
0.75	0.5	RBA	11.6178433
1	0.5	BDH	15.50784949
1.25	0.5	BDH	19.93813003
1.5	0.5	BDH	25.08343949
0.25	0.25	RBA	2.159119023
0.5	0.25	RBA	5.676990818
0.75	0.25	RBA	9.454714141
1	0.25	ABDC	13.3412041
1.25	0.25	ABDC	17.88023421
1.5	0.25	CDG	23.11729814
1.75	0.25	CDG	29.02737902
2	0.25	DHJG	35.58939034
2.25	0.25	DHJG	42.83455324
0.25	0	RBA	1.604742638
0.5	0	RBA	4.318238048
0.75	0	RBA	7.70782377
1	0	ABDC	11.58250658
1.25	0	ABDC	16.25007195
1.5	0	CDG	21.6306627
1.75	0	CDG	27.6978691
2	0	CDG	34.37285187
2.25	0	DHJG	41.61076064
2.5	0	DHJG	49.49276674
0.5	−0.25	RBA	3.581260248
0.75	−0.25	ABDC	6.586958796
1	−0.25	ABDC	10.51697534
1.25	−0.25	CDG	15.18669682
1.5	−0.25	CDG	20.77533982
1.75	−0.25	CDG	26.95853697
2	−0.25	CDG	33.73423273
2.25	−0.25	CDG	41.03615518
2.5	−0.25	DHJG	48.87906376
2.75	−0.25	DHJG	57.36645429
0.25	−0.5	NAC	1.554376386
0.5	−0.5	CDG	3.423955161
0.75	−0.5	CDG	6.363966247
1	−0.5	CDG	10.29563675
1.25	−0.5	CDG	15.09673892
1.5	−0.5	CDG	20.65699767
1.75	−0.5	CDG	26.88215328
2	−0.5	CDG	33.69343098
2.25	−0.5	CDG	41.02540555

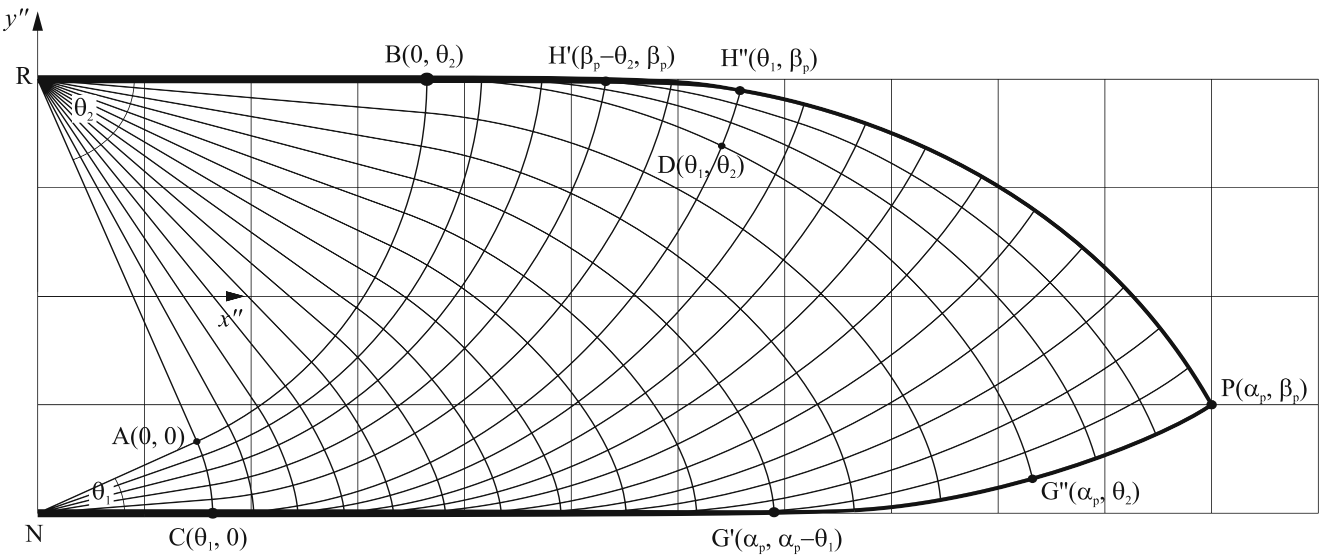

Fig. 4 Case of $\kappa = 5$, $\theta_2 = 0.420534$ rad

and the equation for $v(\mathrm{P})$ is similar; the functions u^*, v^*, $u_\bullet$, $u^\bullet$, $v_\bullet$, $v^\bullet$ are defined as explained above.

4 Selected benchmarks

The aim of this section is to provide the basic characteristics of the optimal cantilevers corresponding to the following values of κ : $1, 2, 3, 5, 7, 9$ and to position of the vertical force $\boldsymbol{P}$ at the grid points: $x''_p = n\frac{a}{4}$, $y''_p = \pm m\frac{a}{4}$, $n = 0, 1, 2, \ldots, 13$; $m = 0, 1, 2$.

Position of nodes A, B, C, D, H, G, J depends on κ, see Fig. 3a–f. The coordinates $(x'', \ y'')$ of these points are set up in Table 1.

For fixed κ and for the subsequent positions of point P, determined by (n, m), we fix the domain in which this point lies, see Tables 2, 3, 4, 5, 6, 7, where the values of x''_p, y''_p are set up in the first two columns and the third column provides the name of the domain. In the last column the volumes of the optimal cantilevers are set up. The two-bar solutions are neglected.

The results set up in Tables 2–7 include the selected results published in Graczykowski and Lewiński (2006c, 2007b).

5 Exemplary result

Consider $\kappa = 5$, $x''_p = 2.75a$, $y''_p = -0.25a$. The division of the feasible domain is shown in Fig. 3d. The coordinates of nodes of this division are given in Table 1. Point P belongs to domain DHJG, $\alpha_p = 1.315713099$ and $\beta_p = 1.408664644$, see Table 5. The layout of the bars is shown in Fig. 4. The volume of this cantilever equals $V = 34.66641774V_0$.

6 Final remarks

The results presented are new; they complement the selected results discussed in the previous papers of the present authors. Let us note that the results published in Srithongchai and Dewhurst (2003) and Gilbert et al. (2005) concern the problem with the feasible domain being a half plane and not a half strip, hence cannot be compared. Nevertheless we have checked that all these results are correct. The authors express their hope that the benchmarks delivered will serve for tests of the currently developed software of the topology optimization problems.

Acknowledgement The paper was prepared within the Research Grant no N506 071338, financed by the Polish Ministry of Science and Higher Education, entitled: *Topology Optimization of Engineering Structures. Simultaneous shaping and local material properties determination*.

Corrigendum to the paper

Graczykowski and Lewiński (2006b) Michell cantilevers constructed within trapezoidal domains—Part II: Virtual displacement fields, *Structural and Multidisciplinary Optimization*, **32** (2006), No 6, 463–471

The second term of the r.h.s. of (6.9) should read:

$$2\kappa^{\frac{3}{2}} F_2(\xi,\ \eta)$$

The first term of the r.h.s. of (6.25) should read:

$$-(\kappa + 2)F_3(\eta,\ \xi)$$

The r.h.s. of (7.1) should read:

$$X^*(\alpha,\ \beta) + X_\bullet(\alpha - \theta_1,\ \beta + \theta_1) + X^\bullet(\alpha + \theta_2,\ \beta - \theta_2)$$

The fifth term of the r.h.s. of (7.2) should read:

$$-(\kappa + 2)F_3(\eta - \theta_2,\ \xi + \theta_2)$$

These misprints do not affect the further results of this paper.

References

Carathéodory C, Schmidt E (1923) Über die Hencky-Prandtlschen Kurven. Z Angew Math Mech 3:468–475

Gilbert M, Darwich W, Tyas A, Shepherd P (2005) Application of large-scale layout optimization techniques in structural engineering practice. In: 6th world congress of structural and multidisciplinary optimization, Rio de Janeiro, Brasil, 30 May–3 June 2005

Graczykowski C, Lewiński T (2006a) Michell cantilevers constructed within trapezoidal domains—part I: geometry of Hencky nets. Struct Multidisc Optim 32(5):347–368

Graczykowski C, Lewiński T (2006b) Michell cantilevers constructed within trapezoidal domains—part II: virtual displacement fields. Struct Multidisc Optim 32(6):463–471

Graczykowski C, Lewiński T (2006c) Force fields within Michell-like cantilevers transmitting a point load to a straight support. In: Bendsøe M, Olhoff N, Sigmund O (eds) IUTAM symposium on topological design optimization of structures, machines and materials. Status and perspectives. Series: solid mechanics and its application, vol 137. Springer, Dordrecht, pp 55–65

Graczykowski C, Lewiński T (2007a) Michell cantilevers constructed within trapezoidal domains—part III: force fields. Struct Multidisc Optim 33:27–46

Graczykowski C, Lewiński T (2007b) Michell cantilevers constructed within trapezoidal domains—part IV: complete exact solutions of selected optimal designs and their approximations by trusses of finite number of joints. Struct Multidisc Optim 33:113–129

Hemp WS (1973) Optimum structures. Clarendon, Oxford

Lewiński T, Zhou M, Rozvany GIN (1994a) Extended exact solutions for least-weight truss layouts-Part I: Cantilever with a horizontal axis of symmetry. Int J Mech Sci 36:375–398

Lewiński T, Zhou M, Rozvany GIN (1994b) Extended exact solutions for least-weight truss layouts- Part II: Unsymmetric cantilevers. Int J Mech Sci 36:399–419

Prager W (1959) On a problem of optimal design. In: Olszak WW (ed) Red., Proc IUTAM symp non-homogeneity in elasticity and plasticity. Pergamon Press, London, pp 125–132

Rozvany GIN (1997) Some shortcomings in Michell's truss theory. Struct Optim 12:244–250 (1996); 13:203–204 (1997)

Srithongchai S, Dewhurst P (2003) Comparisons of optimality criteria for minimum-weight dual material structures. Int J Mech Sci 45:1781–1797